ACS APPLIED MATERIALS & INTERFACES

Research Article

Cite This: ACS Appl. Mater. Interfaces 2018, 10, 12424−12430

www.acsami.org

Facile Biofabrication of Heterogeneous Multilayer Tubular Hydrogels by Fast Diffusion-Induced Gelation

Liliang Ouyang,[†,∥] Jason A. Burdick,[‡] and Wei Sun*[,†,§]

[†]Department of Mechanical Engineering, Tsinghua University, Beijing 100084, China

[‡]Department of Bioengineering, University of Pennsylvania, Philadelphia, Pennsylvania 19104, United States

[§]Department of Mechanical Engineering and Mechanics, Drexel University, Philadelphia, Pennsylvania 19104, United States

Supporting Information

ABSTRACT: Multilayer (ML) hydrogels are useful to achieve stepwise and heterogeneous control over the organization of biomedical materials and cells. There are numerous challenges in the development of fabrication approaches toward this, including the need for mild processing conditions that maintain the integrity of embedded compounds and the versatility in processing to introduce desired complexity. Here, we report a method to fabricate heterogeneous multilayered hydrogels based on diffusion-induced gelation. This technique uses the quick diffusion of ions and small molecules (i.e., photoinitiators) through gel−sol or gel−gel interfaces to produce hydrogel layers. Specifically, ionically (e.g., alginate-based) and covalently [e.g., gelatin methacryloyl (GelMA-based)] photocross-linked hydrogels are generated in converse directions from the same interface. The ML (e.g., seven layers) ionic hydrogels can be formed within seconds to minutes with thicknesses ranging from tens to hundreds of micrometers. The thicknesses of the covalent hydrogels are determined by the reaction time (or the molecule diffusion time). Multiwalled tubular structures (e.g., mimicking branched multiwalled vessels) are mainly investigated in this study based on a removable gel core, but this method can be generalized to other material patterns. The process is also demonstrated to support the encapsulation of viable cells and is compatible with a range of thermally reversible core materials (e.g., gelatin and Pluronic F127) and covalently cross-linked formulations (e.g., GelMA and methacrylated hyaluronic acid). This biofabrication process enhances our ability to fabricate a range of structures that are useful for biomedical applications.

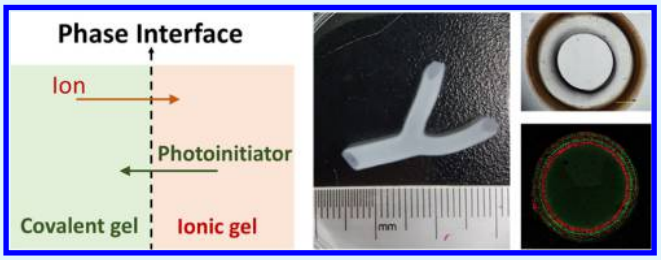

KEYWORDS: *hydrogel cross-linking, multilayer hydrogels, heterogeneity, cell encapsulation, interface diffusion*

1. INTRODUCTION

As a primary class of biomaterials, hydrogels are widely used in biomedical fields for their high water content, ability to entrap viable cells and hydrophilic cargos, and extracellular matrix-like mechanical, physical, and biochemical properties.[1,2] The architecture and geometry of hydrogels are critical for their corresponding applications. Particularly, multilayer (ML) hydrogels in different geometries, such as sandwich-,[3,4] onion-,[5,6] and vessel-like[7−10] structures, are used in numerous biomedical applications, including cell culture/co-culture,[11,12] drug delivery,[13,14] cell-based therapy,[15] and tissue engineering.[16] For instance, multishelled spherical hydrogels showed stepwise release of molecules and multiwalled tubular hydrogels mimicked native vessels in terms of their ML features.

In the last decade, there has been considerable investigation into the fabrication of ML hydrogels. Ladet et al.[17] pioneered this area with the preparation of multimembrane polyelectrolyte alcohol gels (chitosan or alginate (Alg)) from the outside toward the core based on a multistep interrupted neutralization process. However, their multimembrane hydrogels are limited to single types of hydrogels and may be challenging for the loading of viable cells and drugs, considering the basic or acidic environments. Similarly, Xiong et al.[18] reported a pH-triggered inward growing method to generate a ML chitosan polyelectrolyte structure based on chitosan−Alg capsules with chitosan solutions inside. pH-induced gelation was also used for cellulose to prepare ML tubular structures through reloading acetic acid into gel rods layer-by-layer with an outward coating process.[19]

Alg-based ionic gelation is another popular formulation technique to fabricate ML hydrogels because of the fast cross-linking, good biocompatibility, and desirable mechanical properties of Alg hydrogels.[20,21] Dai et al.[22] immersed an Alg core loaded with excess Ca^{2+} into Alg solutions to generate gel layers, and incomplete or complete cross-linking options were provided to obtain ML gels with or without interlayer space; Lin et al.[23] used a similar process but added cellulose nanocrystals into the Alg core for sustained drug release because of the "nano-obstruction effect" and "nanolocking effect"; and Wilkens et al.[10] and Ghanizadeh Tabriz et al.[9]

Received: December 23, 2017
Accepted: March 27, 2018
Published: March 27, 2018

DOI: 10.1021/acsami.7b19537
ACS Appl. Mater. Interfaces 2018, 10, 12424−12430

cyclically dipped a metal rod template into Alg and Ca^{2+} (or Ba^{2+}) solutions to fabricate single ML tubes with or without adding supplements to Alg. Recently, a swelling-induced gelation process was introduced to generate hydrogel films, but this process failed to form MLs.[24] Despite these considerable advances, there is still a great need for feasible ML hydrogel processing techniques that incorporate viable cells. More importantly, there still remains a significant challenge to achieving heterogeneity in loaded cargos and even hydrogel types, which was rarely mentioned by these studies.

Here, we introduce a facile and fast fabrication method to prepare ML hydrogels with heterogeneous and hollow features. Briefly, both an ionic cross-linking based outward growth process and a photocross-linking (PC) based inward growth process were developed using the diffusion of ions or photoinitiator, respectively. For the outside ionic hydrogels, a thermally reversible gel core loaded with Ca^{2+} was immersed successively into Alg solutions, where different cargos (e.g., viable cells) could be supplemented to achieve heterogeneous distribution in different layers. In this process, no additional cross-linkers (e.g., Ca^{2+}) were reloaded between two layers as others have done[6,19,22,23] and we found that up to seven layers of hydrogels with distinct boundaries could be fabricated within 2−3 min. Cell encapsulation was confirmed with controlled distribution across layers. The gel core was optionally dissolvable afterward through changing temperature. To make the inside covalent hydrogels, photocross-linkable formulations were added into the core and the photoinitiator was loaded in the Alg solution used in previous steps. After the generation of outer ionically cross-linked layers, the inner photocross-linked layer was created with the inward diffusion of photoinitiator and the presence of ultraviolet (UV) light. The uncross-linked core was again optionally removable through temperature control. These approaches are useful for various biomedical applications, such as in vascular tissue engineering with complex geometries.

2. MATERIALS AND METHODS

2.1. Materials. Gelatin (type A), Pluronic F-127 (F-127), and sodium Alg were purchased from Sigma-Aldrich, and hyaluronic acid (HA, 75 kDa) was purchased from Lifecore. Gelatin methacryloyl (GelMA) was synthesized through the conjugation of methacrylic anhydride (MA, Sigma-Aldrich) to gelatin as described previously. Briefly, gelatin was dissolved in phosphate buffered saline (PBS) at 60 °C, and MA (0.8 mL per gram of gelatin) was added dropwise, followed by 3 h of reaction at 60 °C under stirring. Methacrylated HA (MeHA) was prepared by esterification between HA and MA, where 3 equiv MA was added dropwise to aqueous 1 wt % HA solution on ice for 6−8 h while adjusting the pH to 8. After overnight reaction at 4 °C, the mixture was neutralized to pH ≈ 7−7.5. After dialysis and lyophilization, both GelMA and MeHA were stored at 4 °C until use. The modifications of GelMA and MeHA were confirmed with ^{1}H NMR as ∼50 and ∼24%, respectively.[25] All of the hydrogel materials, as well as the I2959 photoinitiator and calcium chloride ($CaCl_2$) ionic cross-linker were dissolved in deionized (DI) water, unless otherwise stated.

2.2. Preparation of Multilayer Ionic Hydrogels. A thermally reversible gel core was fabricated and then coated with ionically cross-linked hydrogels. First, a $CaCl_2$-containing gelatin solution was poured into a mold with the desired pattern and subsequently placed at 4 °C for 20 min for gelation. Molds included a disposable 0.5 mL syringe to fabricate simple gel rods, and custom molds using three-dimensional (3D) printing technology to generate complex gel structures (e.g., branched). A fused deposition modeling 3D printer (Raise3D N2) was used to fabricate the custom molds based on polylactic acid filaments. After gelation, the gelatin gel was carefully removed from the mold and then immersed in an Alg solution for coating. The coating reaction was quenched by separating the gel core from the Alg solution, and then, additional layers were introduced by immersing in Alg solution again. The gel was immersed in DI water for 10 s between two reaction periods to avoid possible dehydration. After coating, the ends of the gel were cut off and the sample was placed at 37 °C for 30 min to dissolve the gelatin core. Unless otherwise stated, 7.5% gelatin, 2% $CaCl_2$, and 2% Alg were used, and the coating reaction was performed at room temperature (RT ≈ 24 °C). The reaction time for each layer was set to 10 s to 10 min. When using F-127 as the gel core materials, 40% F-127 containing 2% $CaCl_2$ was treated with 37 and 4 °C for gelation and dissolving, respectively.

2.3. Preparation of Heterogeneous Ionic-Covalent Hydrogels. To fabricate structures with both ionic and covalent hydrogels, the same process as described above was performed, except that gelatin was replaced with GelMA as the gel core material for covalent cross-linking and I2959 was added into the Alg solution. After the coating of one layer of Alg, the gels were immersed in DI water and immediately treated with UV light (wavelength 365 nm, intensity 15 mW/cm^2). Optionally, the gels were held for some time before UV treatment, which altered the final covalent cross-linked hydrogel layer because the thickness of the covalent cross-linked layer was due to the photoinitiator diffusion. The gels were then placed at 37 °C for 30 min to dissolve the unreacted core. Unless otherwise stated, 7.5% GelMA and 0.05% I2959 were used, and the UV treatment time was set from 1 to 6 min. In some cases, 5% gelatin + 5% GelMA or 5% gelatin + 2.5% MeHA were applied as the photocross-linkable gel core materials for further generalization.

2.4. Hydrogel Characterization. The generated hollow hydrogel structures were imaged using microscopy (Olympus CX40 and Nikon TS100-F). To better demonstrate the ML and hollow features, the hydrogel tubes were cut into short rings and the rings were placed on their side to capture the cross section. Both longitudinal and cross-sectional images of the tube walls were used to quantify the layer thickness (four random views for each measurement). Scanning electron microscopy (SEM, FEI Quanta 200) observation was carried out to further investigate the adhesion of hydrogel layers. Hydrogel samples were immersed in DI water and frozen at −80 °C to maintain the integrity, followed by full lyophilization. The samples were then sputtered with gold for observation and photography. Tensile testing of tubular structures, prepared using a 0.5 mL syringe mold, were performed on a mechanical testing instrument (Bose) with a precise force sensor (250 g as limit) and speed of 0.05 mm/s. Young's moduli were determined under strains from 0 to 30% (n = 3). Perfusion of the branched hollow tubes was visualized by perfusing water containing a food dye through the input port.

2.5. Cell Encapsulation and Characterization. Cells were suspended in the Alg solution at a final density of 2.5 × 10^6 cells/mL. For heterogeneous encapsulation of cells, the gel core was immersed into the Alg solutions loaded with different types of cells. To better visualize the cell distributions, cells were tracked with either green or red fluorescence (CellTracker, Thermo Fisher Scientific) and imaged using laser scanning confocal microcopy (Nikon, Z2). Cell viability was determined by live/dead staining, where cell-laden hydrogels were immersed into the staining working solution (1 μM calcein-AM + 2 μM propidium iodide) for 15 min before imaging.

Human umbilical vein endothelial cells (HUVECs) were cultured in an endothelial growth medium, whereas rabbit artery smooth muscle cells (SMCs), NIH 3T3 fibroblasts, and C2C12 cells were cultured in Dulbecco's modified Eagle's medium supplemented with 10% fetal bovine serum and 1% penicillin−streptomycin. All cells were purchased from the National Infrastructure of Cell Line Resource of China.

3. RESULTS AND DISCUSSION

3.1. Diffusion-Induced Gelation of Ionic Hydrogels. The general approach for diffusion-induced gelation for Alg

DOI: 10.1021/acsami.7b19537
ACS Appl. Mater. Interfaces 2018, 10, 12424−12430

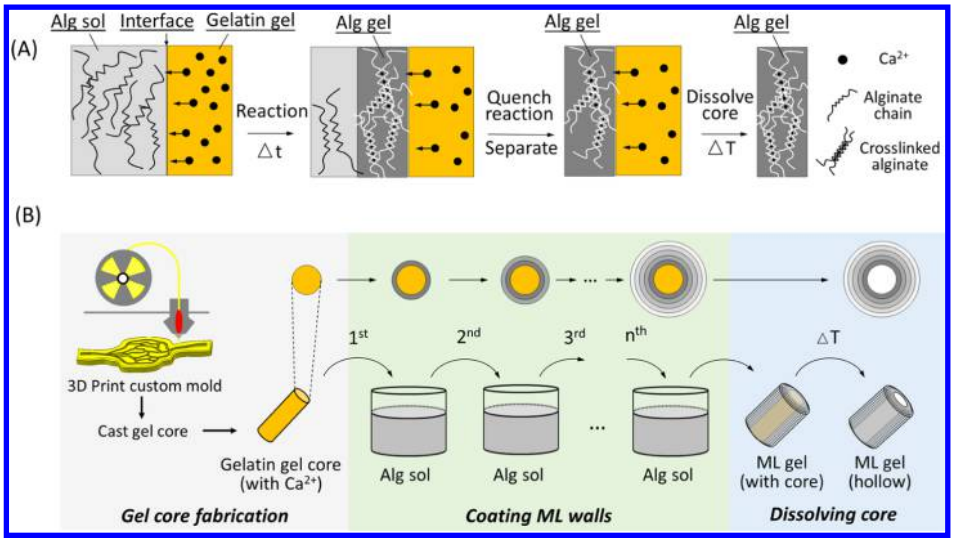

Figure 1. Schematic of ML Alg hydrogel fabrication process. (A) Mechanism of diffusion-induced gelation through the sol−gel interface. (B) Fabrication process consisting of coating ML walls and dissolving the thermally reversible gelatin core.

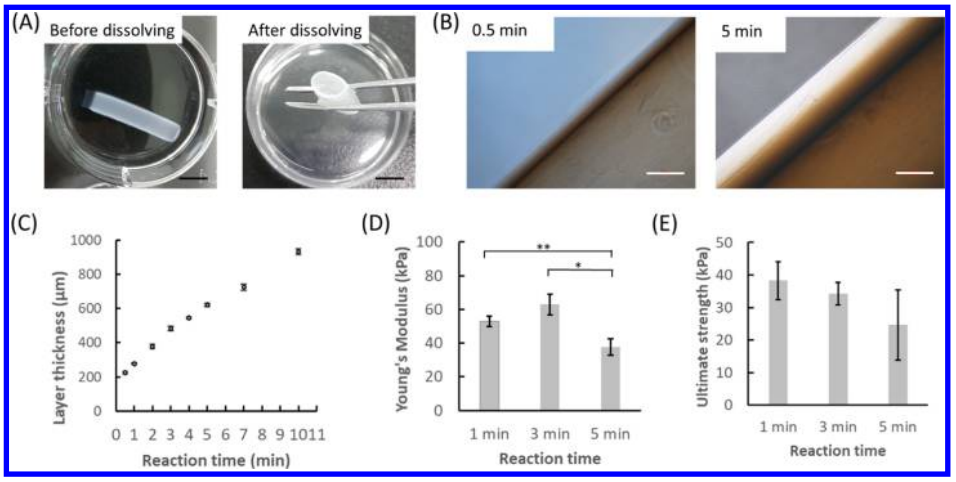

Figure 2. Demonstration of diffusion-induced gelation. (A) Coating of an Alg layer on gelatin gel rod (~5 mm in diameter) before and after dissolving the rod core. (B) Microscopy images of the coated Alg layer (longitudinal direction) under 0.5 and 5 min of contacting time between the gelatin gel rod and the Alg solution, which is also termed reaction time. (C) Alg gel layer thickness with variations in reaction. (D) Young's moduli and (E) yield strengths of the Alg tubular structures under tensile test. Statistical significance was defined as $*p < 0.05$, $**p < 0.01$, $***p < 0.001$ using one-way analysis of variance in conjugation with a Bonferroni posthoc test. Scale bar: (A) 5 mm, (B) 500 μm.

hydrogels is schematically shown in Figure 1A. It was thought that the diffusion of Ca^{2+} from the gelatin gel phase to the Alg sol phase would initiate rapid ionic cross-linking to form Alg layers on the gelatin core. As indicated in Figure 2A, after immersing in Alg solution for 3 min, the gelatin core was coated with a uniform hydrogel layer. The gelatin core was then dissolved with an increase in temperature to leave a hollow tube, which is shown through microscopy images (Figure 2B). The generated layer thickness was dependent on the time of ionic cross-linking, shown in images for both 0.5 and 5 min reaction times (Figure 2B) and quantified for up to 10 min (Figure 2C). Specifically, the layer thickness increased from ~220 to ~930 μm when the reaction time was increased from 0.5 to 10 min. Considering the fast gelation of Alg with Ca^{2+} (occurs within seconds), the layer thickness was controlled by the distance that Ca^{2+} diffuses beyond the interface, and thus the duration that the two phases are in contact.[22]

Apart from the reaction time, there are other factors that affect the coating process. For example, the layer thickness slightly decreased from ~620 to ~460 μm with the increase of the Alg concentration from 0.5 to 3%, and the generated hydrogel layer was optically denser under higher Alg concentration (3%) (Figure S1). A more concentrated Alg solution might reduce the diffusion of Ca^{2+} and thus give rise to thinner gelation. Additionally, the $CaCl_2$ concentration influences the layer thickness, with thicker layers formed at higher Ca^{2+} concentrations because of more Ca^{2+} diffusion (Figure S2). When no Ca^{2+} was included in the gelatin gel (Figure S2A), no hydrogel layer was observed at the interface. Last, it was observed that higher temperatures (i.e., 40 °C) resulted in thicker layers, likely because of the higher activity of Ca^{2+} diffusion at higher temperatures (Figure S3). Overall, any factors that influence Ca^{2+} diffusion and cross-linking influence the layer thickness, such as the reaction time and temperature and Alg and Ca^{2+} concentrations illustrated here.

The mechanical properties of the coated gel layers were determined by a tensile test (Figure S4A). As indicated in the stress−strain curve (Figure S4B), the coated Alg gel was quite

DOI: 10.1021/acsami.7b19537
ACS Appl. Mater. Interfaces 2018, 10, 12424−12430

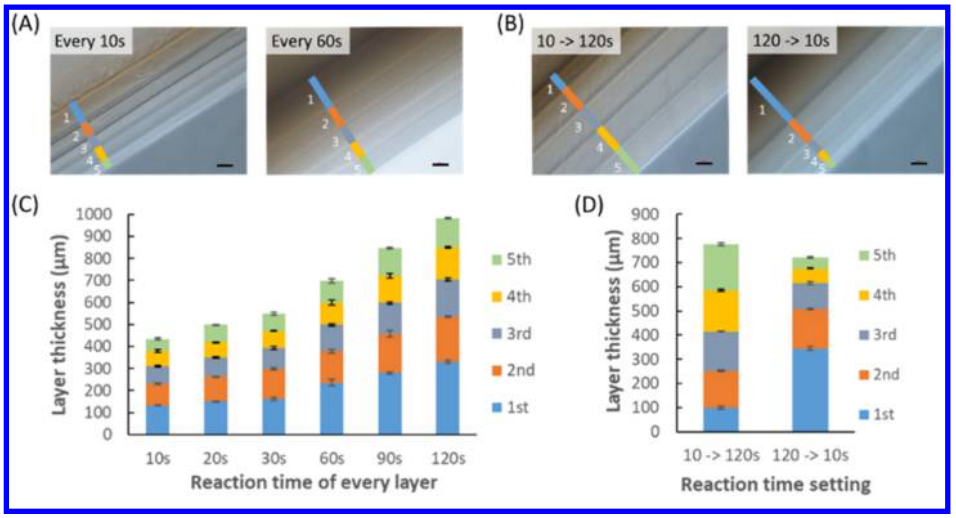

Figure 3. ML Alg hydrogels. Representative microscopy images of five-layer Alg hydrogels (A) under 10 and 60 s of reaction time for each layer, as well as (B) under either increasing or decreasing reaction times for each layer (10, 20, 30, 60, 90, and 120 s for the first, second, third, fourth, and fifth layer, or the reverse). Quantified layer thicknesses under (C) uniform reaction times and (D) increasing and decreasing reaction times. Scale bar: (A,B) 100 μm.

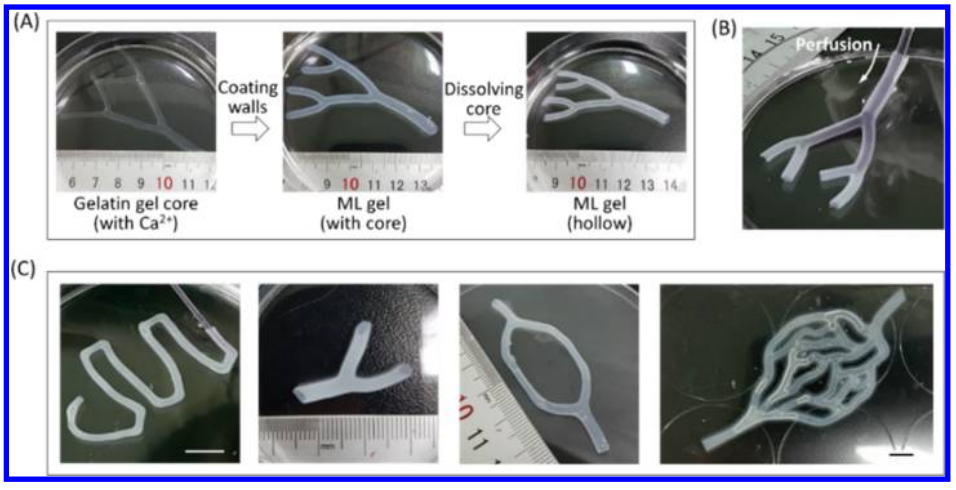

Figure 4. Complex hollow hydrogel structures. (A) Process of fabricating a quadrifurcate vasculature-like structure, consisting of the coating of a gelatin core and subsequent dissolving of the core. (B) Demonstration of perfusion through the hollow channels. (C) Examples of fabricated hollow hydrogel structures, including tortuous single-channel, bifurcate, and connecting tubular structures. Scale bar: (C) 5 mm.

elastic (linear slope) before failure, with an elongation ratio of ~65%. The Young's modulus of the tubular structures under reaction times of 1 and 3 min were ~53 and ~63 kPa, respectively, which were significantly higher than the modulus (~37 kPa) at 5 min (Figure 2D). The ultimate strength decreased slightly with the increasing reaction time (Figure 2E). This might be due to the heterogeneous gelation from inside toward the outside based on ion diffusion; the closer to the core, the higher the degree of gelation is and thus higher is the modulus under shorter reaction times (e.g., 1 or 3 min).

3.2. Multilayer Ionic Hydrogels. As schematically illustrated in Figure 1B, an approach was developed to fabricate ML ionic hydrogel tubes by cyclic immersing of a gel core into an Alg solution. This approach was successful in fabricating layered structures with clear interfaces (Figure 3A,B). As studied above, the diffusion of Ca^{2+} is affected by many parameters, including the reaction time through the length of immersion in the Alg solution (Figure 3A,C). When the same reaction time was used for each layer, the inner layers were thicker than the outer layers; for example, for 10 s reaction times, the thicknesses were 120, 100, 80, 65, and 50 μm for the first−fifth layers, respectively. The thickness varied as the diffusion of Ca^{2+} decreased in the outer layers, as the inner layers consumed ions first. In a previous study fabricating Alg multimembranes based on a cross-linked Alg core,[22] researchers observed that it took tens of minutes to fully cross-link the membrane and they reloaded Ca^{2+} for each layer coating. Herein, we observed that a continuous coating occurred within seconds to minutes. Optionally, the reaction time settings can also be varied to further control the thickness of each layer (Figure 3B,D). Specifically, the first layer was 100 μm thinner than the fifth layer when the reaction time was increased from 10 to 120 s. These results demonstrate that the layer thickness can be altered by changing the reaction time. Though gelatin was mainly used as a thermoreversable gel core formulation, Pluronic F127 was also able to support the ML fabrication process (Figure S9A).

The size and shape of the hollow hydrogel structures are determined by the geometry of the thermally reversible gel core. Small tubular hydrogels (1−3 mm in diameter) were

DOI: 10.1021/acsami.7b19537
ACS Appl. Mater. Interfaces 2018, 10, 12424−12430

successfully fabricated by using smaller gel cores (Figure S5A), where the formation of MLs (seven layers) was still possible (Figure S5B) with layer dimensions as small as ~25 μm in thickness (Figure S5C). Various complex hollow structure designs were possible with this fabrication process by changing the gel core shape, including a quadrifurcate vasculature-like structure as an example (Figure 4). The hollow structure replicated the core structure in geometry (Figure 4A) and could be perfused to confirm the connectivity among branches (Figure 4B and Movie S1). Technically, any vasculature network can be fabricated as long as the required dissolvable gel core can be fabricated, including tortuous single-channel, bifurcating, and connecting tubular structures as examples (Figures S6 and 4C). The combination with 3D printing technology greatly enhances the ability of this approach in terms of geometric complexity, considering typically studied tubular structures.[9,10,17,19]

To ensure that the layers are maintained with these complex and branching patterns, layers were imaged in fabricated hollow structures and observed to be maintained even at the sites of branching (Figure S7A). In further quantification of layer thickness at different positions along the walls, the wall thickness was ~600 μm (every layer ~200 μm) for all of the straight positions (Figure S7B); however, the branching positions presented thicker walls, especially with larger turning angles (turning angle was defined as the included angle between the extension path and turning path as indicated in Figure S7A)—the wall thickness of 113° and 51° turning positions were ~830 and ~700 μm, respectively. This can be explained by the cross diffusion of ions from angled interfaces, which increases the extent of ion diffusion and cross-linking and leads to thicker hydrogels. Despite this difference, the branched hollow structures presented good fidelity and uniform geometry as a whole.

3.3. Diffusion-Induced Gelation of Covalent Hydrogels. The generation of covalent hydrogel layers was designed on the other side of the interface, building from the previously described ML ionic system. As illustrated schematically (Figure 5A), a photoinitiator is now included in the Alg solution, so that there is simultaneous formation of the Alg layer (from diffusion of Ca^{2+} into the Alg solution) and diffusion of the photoinitiator into the reversible GelMA gel. With subsequent UV treatment, areas where the photoinitiator is present will be covalently cross-linked in the GelMA because of radical polymerization of included methacrylate groups. Any unreacted GelMA is then removed through an increase in temperature (Figure 5B). To demonstrate this process, the generated Alg walls were either retained or peeled off to avoid possible further input of the photoinitiator. In both cases, GelMA layers (~350 μm in thickness) were formed after 2.5 min UV irradiation, followed by dissolving the unreacted gel core (Figure S8B). This result indicates that the covalent layers are formed through photoinitiator diffusion and presents the opportunity to control the heterogeneous structures through control of the photoinitiator diffusion. The diffusion of ions, small molecules, and macromolecules is controlled through the diffusing phase (e.g., solution and hydrogel).[22,26−28] This work demonstrates that both Ca^{2+} ions and small molecule photoinitiators can diffuse from a gel phase into a sol phase or another gel phase, which is useful to continuously generate hydrogel layers.

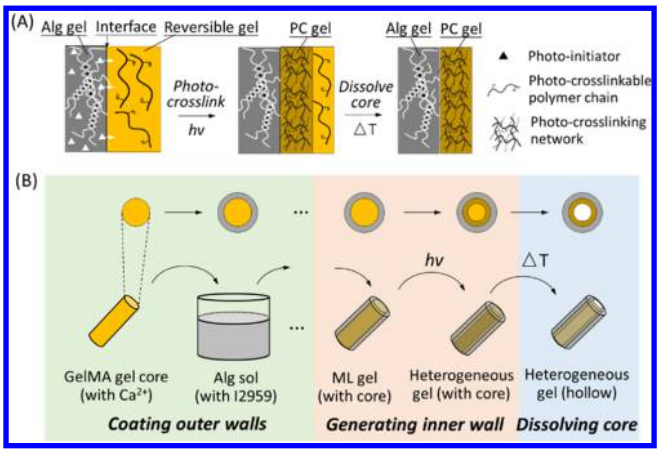

Figure 5. Schematic of heterogeneous ionic-covalent hydrogel fabrication. (A) Mechanism of diffusion-induced PC through the gel−gel interface. (B) Fabrication process consists of coating the GelMA core with an outer Alg layer, generating an inner PC wall, and dissolving the unreacted portion of the thermally reversible core.

3.4. Heterogeneous Ionic-Covalent Hydrogels. When leaving the outer Alg gel with the inner gel core, it is possible to obtain heterogeneous ionic-covalent hollow hydrogels. Figure 6A shows microscopy images of heterogeneous hydrogels treated with different UV irradiation times. The two layers of Alg gel and PC gel consist of standard concentric circles in the cross section with a clear interface. Furthermore, the PC gel thickness increased with the UV treatment time—the PC gel was ~830 and ~310 μm in thickness under 6 and 1 min UV irradiation, respectively (Figure 6B). This is similar to the ionic hydrogel generation in terms of reaction time influence on molecule diffusion.

To further investigate the growth of the covalent layer, the hydrogels (coated Alg gel + inner gel core) were held for various times before UV irradiation (Figure S8A). As expected, the thickness of the PC layer increased with the holding time (under the same UV irradiation time 2.5 min) (Figure S8C). After holding for 10 min, the inner lumen was hardly visible, because of extensive photoinitiator diffusion and subsequent reaction. The results indicate that the photoinitiator diffusion happens during static contacting with Alg gel and that the diffusion is based on the time of contact to generate heterogeneous layers (Figure S8A). Though 7.5% GelMA was mainly studied as the photocross-linkable and reversible formulation for gel core, other formulations (e.g., 5% gelatin + 5% GelMA and 5% gelatin + 2.5% MeHA) were also tested to be possible to form ionic-covalent tubular hydrogels (Figure S9B,C), which meant potential diversity of applicable materials with this approach.

Coadhesion between heterogeneous hydrogels with different cross-linking mechanisms is an important consideration. Figure 6C shows the microscopy and SEM images of the ionic covalent hydrogels after immersing in PBS for 12 h. It is clearly observed that the inner PC gel and the outer Alg gel are separated from each other, leaving a distinct gap (red arrows). This may be caused by the lack of coadhesion and different swelling ratios for the two gels or as artifact because of the drying process. The applied ionic cross-linking and PC are examples of physical and chemical cross-linkings, respectively; thus, there is no connection between the two networks. When 2.5 wt % GelMA was added in the Alg solution to provide a uniform covalent structure across the layers, the layers adhered quite well, forming a tubular structure (Figure 6D). The SEM image confirmed the improved coadhesion between the

DOI: 10.1021/acsami.7b19537
ACS Appl. Mater. Interfaces 2018, 10, 12424−12430

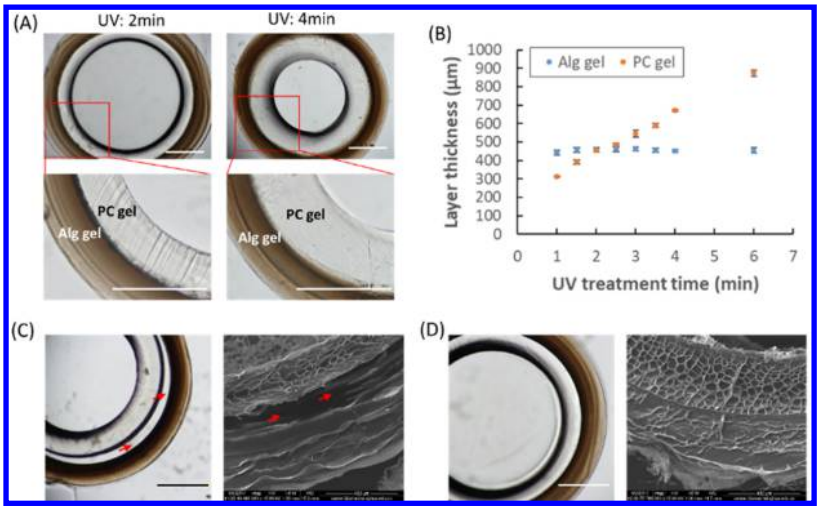

Figure 6. Heterogeneous hollow hydrogel channels. (A) Cross-sectional images of heterogeneous hollow tube under UV treatment time of 2 and 4 min. (B) Quantification of Alg and covalent layer thicknesses with changes in UV treatment time. Microscopy and SEM images of the cross section for samples (C) without or (D) with photocross-linkable components in the Alg solution. Red arrows in (C) indicate delamination between the various layers, which is not observed in (D). Scale bar: (A) 1 mm, (C,D) 1 mm (left) and 400 μm (right).

heterogeneous gels, a result of this covalent cross-linking across the two layers. The successful combination of two different types of hydrogels introduces possibilities in heterogeneity when compared with ML hydrogels of a single material.[17−19,22,23]

3.5. Cell Encapsulation. As mentioned above, it is important that the fabrication process is amenable to the encapsulation of viable cells to expand the applicability of the fabrication process to numerous biomedical applications. Thus, the various materials and reactions were selected because of their previous use in the incorporation of viable cells. As shown in Figure 7A, five layers of cells marked with alternate green/red fluorescence were assembled in a layer-by-layer fashion into a tubular structure, by immersing the core gel into alternating solutions of each labeled cells. The cells in each layer were separated through distinct boundaries, indicating limited mixing of the gel components at each step. To illustrate the ability to layer different cell types, heterogeneous ML cell-laden tubes (~1.5 mm in diameter) were fabricated with HUVECs, SMCs, and fibroblasts distributed from the inside to the outside of tubes, potentially mimicking the native blood vessels (Figure 7B). Furthermore, cell viability was assessed using live−dead staining, which indicated that cell viability (>90%) was high throughout the layers (Figure 7C). Cell encapsulation benefits from the cell-friendly process of this approach, where short durations (within minutes) and low ion (low to 43 mM for Ca^{2+}) and photoinitiator (0.05% for I2959) concentrations are applied. In some existing ML hydrogel systems, higher Ca^{2+} concentrations (e.g., 200 mM) are used for tens of minutes[22,23] and some even introduce acidic or basic environments,[17−19] which might compromise cell viability.

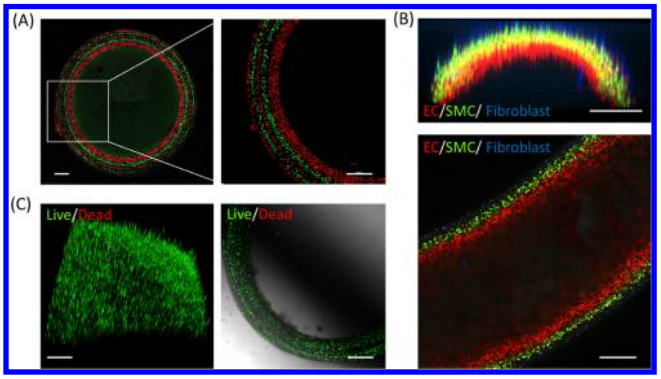

Figure 7. Cell encapsulation with layered hydrogels. (A) Images of a five-layer Alg tube embedded with fluorescence-tracked C2C12 cells of alternating color. (B) Cross-sectional (top) and longitudinal section (bottom) images of a three-layer Alg tube embedded with HUVECs (red), SMCs (green), and fibroblasts (blue) in different layers. (C) 3D reconstruction (left) and cross-sectional (right) images of C2C12 cell-laden ML walls stained for live (green) and dead (red) cells. Scale bar: (A−C) 500 μm.

4. CONCLUSIONS

A facile strategy was developed to fabricate heterogeneous ML hydrogels based on diffusion-induced gelation, which was performed by placing cross-linking reagents (e.g., cross-linker, initiator) and polymers into two different contacting phases. By adding Ca^{2+} in a gel core and immersing it in Alg solution, Alg gel layers were easily generated on the core surface within seconds to minutes, and lumens were formed through dissolution of the gel core. Similarly, a layer of covalently cross-linked GelMA gel was successfully created on the phase interface by adding the photoinitiator to the Alg solution and subsequently cross-linking with light. Branched and hollow features were easily achieved with this approach, and cells were successfully encapsulated into different layers with high viability (>90%). This approach shows great potential in various biomedical areas involving ML hydrogels where complexity of layers and cell placement is desired.

■ ASSOCIATED CONTENT

Supporting Information

The Supporting Information is available free of charge on the ACS Publications website at DOI: 10.1021/acsami.7b19537.

Effect of Alg concentration, Ca^{2+} concentration, and reaction time on Alg layer thickness; tensile testing process and representative stress−strain curve; variety in tubular size and layer numbers; 3D printed molds for gel

DOI: 10.1021/acsami.7b19537
ACS Appl. Mater. Interfaces 2018, 10, 12424−12430

core fabrication; analysis of branched tubular structure with ML feature and cell encapsulation; analysis of PC gel layer formation process; effect of contacting time on OC gel layer thickness; Pluronic F127 as core formulation; and GelMA- and MeHA-containing hybrid materials as PC gel formulations (PDF)
Perfusion demonstration (AVI)

AUTHOR INFORMATION

Corresponding Author

*E-mail: weisun@tsinghua.edu.cn.

ORCID

Liliang Ouyang: 0000-0003-4177-8698
Jason A. Burdick: 0000-0002-2006-332X

Present Address

[‖]Department of Materials, Imperial College London, London, SW7 2AZ, UK (L.O.).

Notes

The authors declare no competing financial interest.

ACKNOWLEDGMENTS

The authors acknowledge the support from Prof. Molly Stevens in mechanical characterization. This study was financially funded by the Natural Science Foundation of China (nos. 51235006 and 31500818), the National Science and Technology Major Projects for New Drug Development (no. 2015ZX09501009), the Beijing Municipal Science & Technology Commission Key Project (no. Z1411000002814003) and Overseas Expertise Introduction Project for Discipline Innovation (111 Project, no. G2017002).

REFERENCES

(1) Lutolf, M. P. Biomaterials: Spotlight on hydrogels. *Nat. Mater.* **2009**, *8*, 451−453.
(2) Malda, J.; Visser, J.; Melchels, F. P.; Jüngst, T.; Hennink, W. E.; Dhert, W. J. A.; Groll, J.; Hutmacher, D. W. 25th anniversary article: Engineering hydrogels for biofabrication. *Adv. Mater.* **2013**, *25*, 5011−5028.
(3) Goodwin, A. M. In vitro assays of angiogenesis for assessment of angiogenic and anti-angiogenic agents. *Microvasc. Res.* **2007**, *74*, 172−183.
(4) Foster, E.; You, J.; Siltanen, C.; Patel, D.; Haque, A.; Anderson, L.; Revzin, A. Heparin hydrogel sandwich cultures of primary hepatocytes. *Eur. Polym. J.* **2015**, *72*, 726−735.
(5) Wei, S. J.; Zhang, M.; Li, L.; Lu, L. Alginate-based multi-membrane hydrogel for dual drug delivery system. *Appl. Mech. Mater.* **2013**, *275*−*277*, 1632−1635.
(6) Duan, J.; Hou, R.; Xiong, X.; Wang, Y.; Wang, Y.; Fu, J.; Yu, Z. Versatile fabrication of arbitrarily shaped multi-membrane hydrogels suitable for biomedical applications. *J. Mater. Chem. B* **2013**, *1*, 485−492.
(7) Shinohara, S.; Kihara, T.; Sakai, S.; Matsusaki, M.; Akashi, M.; Taya, M.; Miyake, J. Fabrication of in vitro three-dimensional multilayered blood vessel model using human endothelial and smooth muscle cells and high-strength PEG hydrogel. *J. Biosci. Bioeng.* **2013**, *116*, 231−234.
(8) Yoshida, H.; Matsusaki, M.; Akashi, M. Multilayered Blood Capillary Analogs in Biodegradable Hydrogels for In Vitro Drug Permeability Assays. *Adv. Funct. Mater.* **2013**, *23*, 1736−1742.
(9) Ghanizadeh Tabriz, A.; Mills, C. G.; Mullins, J. J.; Davies, J. A.; Shu, W. Rapid Fabrication of Cell-Laden Alginate Hydrogel 3D Structures by Micro Dip-Coating. *Front. Bioeng. Biotechnol.* **2017**, *5*, 13.
(10) Wilkens, C. A.; Rivet, C. J.; Akentjew, T. L.; Alverio, J.; Khoury, M.; Acevedo, J. P. Layer-by-layer approach for a uniformed fabrication of a cell patterned vessel-like construct. *Biofabrication* **2016**, *9*, 015001.
(11) Gao, B.; Konno, T.; Ishihara, K. Quantitating distance-dependent, indirect cell-cell interactions with a multilayered phospholipid polymer hydrogel. *Biomaterials* **2014**, *35*, 2181−2187.
(12) Weber, L. M.; Cheung, C. Y.; Anseth, K. S. Multifunctional pancreatic islet encapsulation barriers achieved via multilayer PEG hydrogels. *Cell Transplant.* **2007**, *16*, 1049−1057.
(13) Park, S.; Bhang, S. H.; La, W.-G.; Seo, J.; Kim, B.-S.; Char, K. Dual roles of hyaluronic acids in multilayer films capturing nanocarriers for drug-eluting coatings. *Biomaterials* **2012**, *33*, 5468−5477.
(14) Mehrotra, S.; Lynam, D.; Maloney, R.; Pawelec, K. M.; Tuszynski, M. H.; Lee, I.; Chan, C.; Sakamoto, J. Time Controlled Protein Release from Layer-by-Layer Assembled Multilayer Functionalized Agarose Hydrogels. *Adv. Funct. Mater.* **2010**, *20*, 247−258.
(15) Xue, B.; Wang, W.; Qin, J.-J.; Nijampatnam, B.; Murugesan, S.; Kozlovskaya, V.; Zhang, R.; Velu, S. E.; Kharlampieva, E. Highly efficient delivery of potent anticancer iminoquinone derivative by multilayer hydrogel cubes. *Acta Biomater.* **2017**, *58*, 386−398.
(16) Ravi, S.; Caves, J. M.; Martinez, A. W.; Haller, C. A.; Chaikof, E. L. Incorporation of fibronectin to enhance cytocompatibility in multilayer elastin-like protein scaffolds for tissue engineering. *J. Biomed. Mater. Res., Part A* **2013**, *101*, 1915−1925.
(17) Ladet, S.; David, L.; Domard, A. Multi-membrane hydrogels. *Nature* **2008**, *452*, 76−79.
(18) Xiong, Y.; Yan, K.; Bentley, W. E.; Deng, H.; Du, Y.; Payne, G. F.; Shi, X.-W. Compartmentalized Multilayer Hydrogel Formation Using a Stimulus-Responsive Self-Assembling Polysaccharide. *ACS Appl. Mater. Interfaces* **2014**, *6*, 2948−2957.
(19) He, M.; Zhao, Y.; Duan, J.; Wang, Z.; Chen, Y.; Zhang, L. Fast contact of solid-liquid interface created high strength multi-layered cellulose hydrogels with controllable size. *ACS Appl. Mater. Interfaces* **2014**, *6*, 1872−1878.
(20) Pawar, S. N.; Edgar, K. J. Alginate derivatization: a review of chemistry, properties and applications. *Biomaterials* **2012**, *33*, 3279−3305.
(21) Ouyang, L.; Yao, R.; Mao, S.; Chen, X.; Na, J.; Sun, W. Three-dimensional bioprinting of embryonic stem cells directs high-throughput and highly uniform embryoid body formation. *Biofabrication* **2015**, *7*, 044101.
(22) Dai, H.; Li, X.; Long, Y.; Wu, J.; Liang, S.; Zhang, X.; Zhao, N.; Xu, J. Multi-membrane hydrogel fabricated by facile dynamic self-assembly. *Soft Matter* **2009**, *5*, 1987−1989.
(23) Lin, N.; Gèze, A.; Wouessidjewe, D.; Huang, J.; Dufresne, A. Biocompatible Double-Membrane Hydrogels from Cationic Cellulose Nanocrystals and Anionic Alginate as Complexing Drugs Codelivery. *ACS Appl. Mater. Interfaces* **2016**, *8*, 6880−6889.
(24) Moreau, D.; Chauvet, C.; Etienne, F.; Rannou, F. P.; Corté, L. Hydrogel films and coatings by swelling-induced gelation. *Proc. Natl. Acad. Sci. U.S.A.* **2016**, *113*, 13295−13300.
(25) Ouyang, L.; Highley, C. B.; Sun, W.; Burdick, J. A. A Generalizable Strategy for the 3D Bioprinting of Hydrogels from Nonviscous Photo-crosslinkable Inks. *Adv. Mater.* **2017**, *29*, 1604983.
(26) Reitan, N. K.; Juthajan, A.; Lindmo, T.; de Lange Davies, C. Macromolecular diffusion in the extracellular matrix measured by fluorescence correlation spectroscopy. *J. Biomed. Opt.* **2008**, *13*, 054040.
(27) Wu, Z. L.; Kurokawa, T.; Sawada, D.; Hu, J.; Furukawa, H.; Gong, J. P. Anisotropic Hydrogel from Complexation-Driven Reorientation of Semirigid Polyanion at Ca2+ Diffusion Flux Front. *Macromolecules* **2011**, *44*, 3535−3541.
(28) Branco, M. C.; Pochan, D. J.; Wagner, N. J.; Schneider, J. P. Macromolecular diffusion and release from self-assembled β-hairpin peptide hydrogels. *Biomaterials* **2009**, *30*, 1339−1347.

DOI: 10.1021/acsami.7b19537
ACS Appl. Mater. Interfaces 2018, 10, 12424−12430